Dual-scale visualization of resin flow for liquid composite molding processes

Teixidó, Helena; Caglar, Baris; Michaud, Véronique

Publication date
2022

Document Version
Final published version

Published in
Proceedings of the 20th European Conference on Composite Materials: Composites Meet Sustainability

Citation (APA)
Teixidó, H., Caglar, B., & Michaud, V. (2022). Dual-scale visualization of resin flow for liquid composite molding processes. In A. P. Vassilopoulos, & V. Michaud (Eds.), *Proceedings of the 20th European Conference on Composite Materials: Composites Meet Sustainability: Vol 2 – Manufacturing* (pp. 1013-1020). EPFL Lausanne, Composite Construction Laboratory.

ECCM 20

26-30 JUNE 2022

LAUSANNE SWITZERLAND

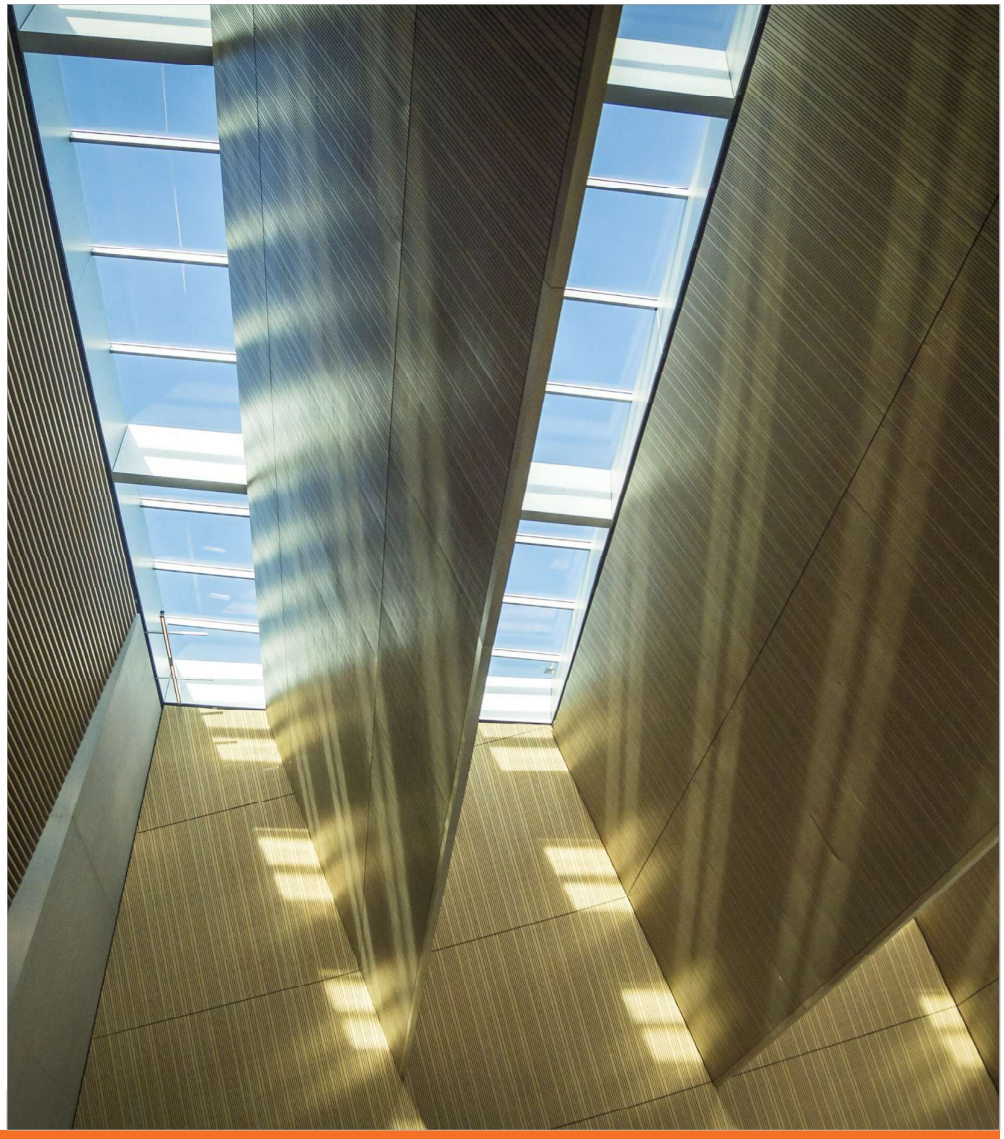

Proceedings of the 20th European Conference on Composite Materials

COMPOSITES MEET SUSTAINABILITY

Vol 2 – Manufacturing

Editors : Anastasios P. Vassilopoulos, Véronique Michaud

Organized by : EPFL CCLAB Composite Construction Laboratory

Under the patronage of : LPAC Laboratory for Processing of Advanced Composites; ESCM EUROPEAN SOCIETY FOR COMPOSITE MATERIALS

ECCM 20
26-30 JUNE 2022
LAUSANNE SWITZERLAND

EPFL CCLAB Composite Construction Laboratory LPAC Laboratory for Processing of Advanced Composites

Proceedings of the 20th European Conference on Composite Materials ECCM20 26-30 June 2022, EPFL Lausanne Switzerland

Edited By :

Prof. Anastasios P. Vassilopoulos, CCLab/EPFL
Prof. Véronique Michaud, LPAC/EPFL

Oragnized by:

Composite Construction Laboratory (CCLab)
Laboratory for Processing of Advanced Composites (LPAC)
Ecole Polytechnique Fédérale de Lausanne (EPFL)

ISBN: 978-2-9701614-0-0
DOI: http://dx.doi.org/10.5075/epfl-298799_978-2-9701614-0-0

Published by :

Composite Construction Laboratory (CCLab)
Ecole Polytechnique Fédérale de Lausanne (EPFL)
BP 2225 (Bâtiment BP), Station 16
1015, Lausanne, Switzerland

https://cclab.epfl.ch

Laboratory for Processing of Advanced Composites (LPAC)
Ecole Polytechnique Fédérale de Lausanne (EPFL)
MXG 139 (Bâtiment MXG), Station 12
1015, Lausanne, Switzerland

https://lpac.epfl.ch

Cover:

Swiss Tech Convention Center
© Edouard Venceslau - CompuWeb SA

Cover Design:

Composite Construction Laboratory (CCLab)
Ecole Polytechnique Fédérale de Lausanne (EPFL)
Lausanne, Switzerland

©2022 ECCM20/The publishers

Disclaimer:

DUAL-SCALE VISUALIZATION OF RESIN FLOW FOR LIQUID COMPOSITE MOLDING PROCESSES

Helena Teixidó[a], Baris Caglar[b], Véronique Michaud[a]

a: Laboratory for Processing of Advanced Composites (LPAC), Institute of Materials (IMX)
Ecole Polytechnique Fédérale de Lausanne (EPFL), 1015 Lausanne, Switzerland
helena.teixidopedarros@epfl.ch
b: Aerospace Manufacturing Technologies, Faculty of Aerospace Engineering, Delft University of Technology, Kluyverweg 1, 2629HS Delft, the Netherlands

Abstract: *Visualization of resin flow progression through fibrous preforms is often sought to elucidate flow patterns and validate models for filling prediction for liquid composite molding processes. Here, conventional X-ray radiography is compared to X-ray phase contrast technique to image in-situ constant flow rate impregnation of a non-translucent unidirectional carbon fabric. X-ray attenuation of the fluid phase was increased by using a ZnI_2-based contrasting agent, leading to enough contrast between the liquid and the low density fibers. We proved the suitability of conventional X-ray transmission to visualize fluid paths by elucidating different flow patterns, spanning from capillary to viscous regimes and a macro-void entrapment phenomenon.*

Keywords: Liquid Composite Molding (LCM); Resin flow; Saturation curve; Process monitoring; X-ray imaging.

1. Introduction

Liquid Composite Molding (LCM) techniques belong to infiltration processes whereby a liquid matrix is forced to flow in between the open pore space of a fibrous reinforcement placed inside a closed mold. Textiles used in composite processing exhibit a highly anisotropic network of pores, generally with a dual scale comprised of intra- and inter-tow spaces resulting in a dual-scale flow leading to a void entrapment mechanism. At the flow front, there is a constant competition between viscous and capillary forces; depending on the extent of viscous/capillary flow and the textile architecture, the fluid pattern as well as the amount of entrapped voids properties will vary. The dimensionless capillary number is used to define the relative influence of viscous and capillary flow regimes:

$$Ca = \frac{u_l \eta}{\gamma_{la}} \quad (1)$$

where u_l, η, and γ_{la} are the fluid velocity, viscosity and surface tension respectively. Researchers converged on the existence of an optimal capillary number for which capillary and viscous forces compensate each other and the amount of the voids is minimal. However, its value is specific for a given resin/fabric system and no one to date has been able to predict it quantitatively (1).

Multiphase flow and progressive saturation of the preforms have received much attention during the past decades with the aim to better understand the flow behavior and predict optimum fibrous preform impregnations (2). In practice, flow studies couple an in-situ flow visualization to mathematical models and numerical simulations to explore unsaturated flows

  doi:10.5075/epfl-298799_978-2-9701614-0-0

and void formation mechanisms. Nevertheless, flow visualization is still a difficult task and often reserved to optically translucent reinforcements such as glass fibers and few studies have been performed on observing flow patterns through non-translucent preforms. One of the proposed methods relies on the inclusion of sensors in-between stacked preforms (3,4). However, imaging techniques that do not require embedding additional materials are in general preferred to detect realistic flow paths. For example, ultrasound techniques (5,6) and Magnetic Resonance Imaging (MRI) have been investigated as potential techniques to visualize dual scale-flows (7). However, either spatial or time resolutions remain the limiting factors.

Nowadays, X-ray based techniques are gaining interest for fluid tracking and analysis given their fast time resolution. Bréard et al. (8) proposed to use conventional X-ray radiography to visualize the ingress of silicon oil into a thick glass preform. However, the low absorption coefficient of carbon and flax limits the resulting contrast with the fluid phase for an accurate liquid/fabric distinction. X-ray micro computed tomography (µCT) systems have enabled the observation of dual-scale flows at unprecedented resolutions (9,10). Recently, Castro el al. (11) used synchrotron radiation computed laminography to image 3D in-situ dual scale flows with micron-scale resolution at an acquisition rate of 1.8 minutes per tomogram. This method allows to locally study void distribution and flow patterns at a small scale when compared to real composite impregnation scales; however, the flow kinetics should remain well below the industrially relevant range.

In Ref. (12), we proposed to use an X-ray phase contrast device (13) to assess the progressive saturation of several distinct fibrous preforms even with conventional resins with acquisition rates below 10 seconds per radiograph. This technique is sensitive to the ultra-small angle scattering and allows to enhance the contrast between materials with low density but with enough microscale heterogeneities. In some cases, a sufficient contrast to elucidate clear flow patterns was not achieved. To overcome this limitation, we explored the use of contrasting agents in the fluid phase to enhance the fluid/fabric contrast in conventional absorption images. The benefits and limitations between the two methods for elucidation of dynamic patterns and entry data for mathematical models are addressed.

2. Materials and Methods

2.1 Materials

The unidirectional carbon fiber reinforcement from Suter Kunststoffe AG (A_w=270 g/m^2), previously employed in Ref. (12) was selected as non-translucent porous media. The fabric contains thin E-glass threads in the weft direction to hold in place and tightly pack carbon tows resulting in inconspicuous space between the tows. Two tests fluids based on an aqueous solution of poly(ethylene glycol) (PEG) (Mw=35 kDa, Sigma Aldrich) were used. The first fluid had a concentration of 16.7 wt% of PEG and in the second one a ZnI_2-based contrasting solution (14) was added to the first solution, resulting in the following formulation: 67.9 wt% of water, 8.2 wt% of PEG, 20.4 wt% of ZnI_2 and 3.5% wt% of Kodak PhotoFlow 200. The properties of the mixtures are listed in Table 1. The viscosity was measured in continuous shear mode in a concentric rheometer (AR2000ex, TA Instrument) by means of a Peltier Couette setup at a constant shear-rate of 10 s^{-1}. The surface tension in air at ambient temperature was assessed by means of the pendant drop method with a Drop Shape Analyzer (DSA30, Krüss).

  doi:10.5075/epfl-298799_978-2-9701614-0-0

Table 1: Properties of tests fluids measured at 20°C.

Fluid	Viscosity [Pa·s]	Density [g/ml]	Surface tension [mN/m]
PEG 16.7%	0.103	1.026	56.5
PEG solution with ZnI_2	0.087	1.276	32.7

2.2 Flow experiments

Flow experiments were performed with the setup from Ref. (12). Fabric layers were accurately hand-cut to a dimension of 4.95 ± 0.05 cm x 15 ± 0.10 cm. Then, nine layers were fitted into the PMMA mold with a 3 mm cavity, leading to a fiber volume fraction of approximatively 45%. A silicon joint was used to prevent race-tracking. Close to the fluid inlet, a Keller Series 35XHTT sensor was placed to monitor the fluid pressure and temperature. Vertical constant flow rate experiments were carried out, the capillary number thus stays constant along the test and the fluid velocity was estimated by measuring the average front velocity. Three experiments were conducted at different flow rates to obtain a range of flow regimes spanning from capillary to viscous dominated. A summary of the experimental campaign is given in Table 2, three flow rates were set and repeated using both fluids.

Table 2: Impregnation experiments.

#	Fluid	Flow front velocity [mm/s]	Ca (10^{-3})
1	PEG 16.67%	0.08	0.15
2	PEG 16.67%	0.26	0.47
3	PEG 16.67%	0.38	0.69
4	PEG solution with ZnI_2	0.08	0.21
5	PEG solution with ZnI_2	0.26	0.69
6	PEG solution with ZnI_2	0.38	1.01

The phase contrast X-ray apparatus developed in (13) was employed to image the flow front for the different tests. As explained in (12), this device allows obtaining three different images: absorption, refraction and scattering images. An imaging area of around 70 mm × 70 mm per acquisition was obtained and the apparatus incorporates a moving platform whose movement can be synchronized with the scanning routine. Image size was 1334 x 1331 pixels and the resulting pixel size about 50 µm. Images were taken at an averaged time of 9.2 s per acquisition and in order to entirely image the impregnation, six different stage positions were defined; then, depending on the fluid speed the number of acquisitions per positions was adapted.

3. Experimental results

3.1 Observation of flow regimes by X-ray phase contrast

Test #1, #2 and #3 correspond respectively to capillary, balanced and viscous flows and the images recorded by X-ray-phase contrast are shown Figure 1. As already reported in (12), the

  doi:10.5075/epfl-298799_978-2-9701614-0-0

higher fabric/fluid contrast is obtained in scattering images. In test #3, viscous fingering and unsaturated length are clearly depicted in the scattering images. Absorption, refraction and scattering images show a rather balanced flow for impregnation #2. However, for experiment #1, although the flow front position is clearly identified in the scattering images, the intra-tow capillary fingering is not elucidated. Absorption and refraction images show a large unsaturated area and a flow preferentially filling the tows, though, the interpretation of the flow front in these images is hampered by the low contrast obtained. To overcome this limit, we thus investigated the potential benefit of a contrasting agent in the solution to increase the effect of the fluid on the attenuation signal and thus observe the flow progression in absorption images.

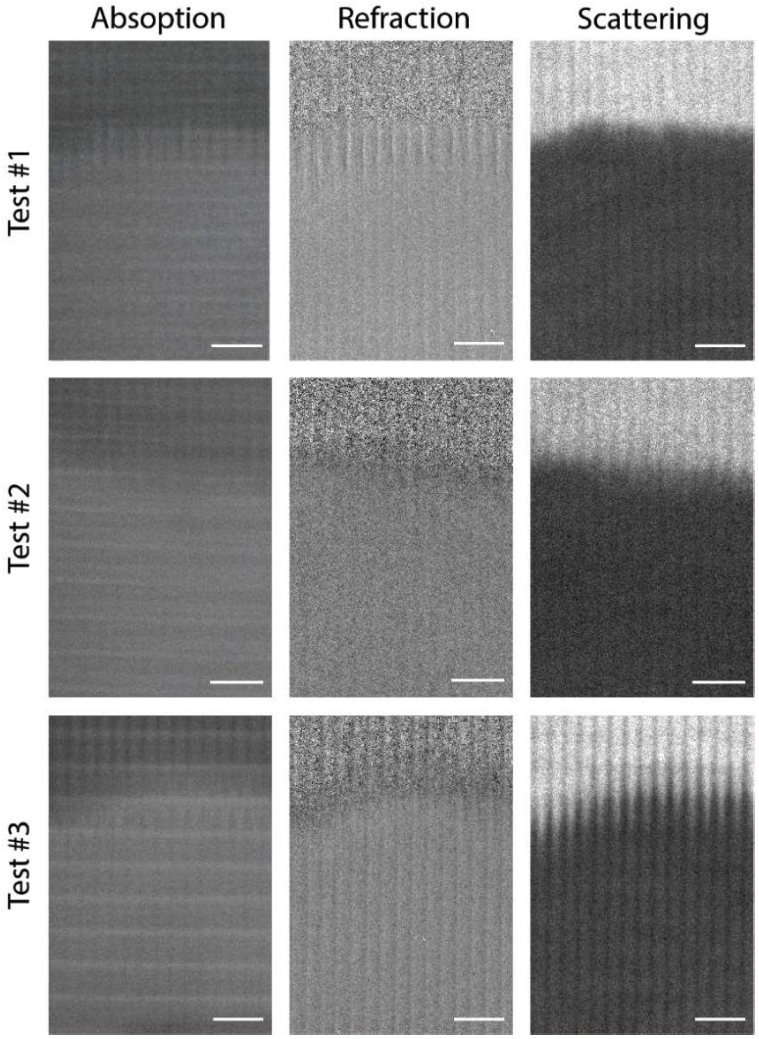

Figure 1. Absorption, refraction and scattering images obtained for tests #1, #2 and #3. The scale bar corresponds to 5 mm.

3.2 Observation of flow regimes by X-ray transmission

Flow front images obtained for experiments #4, #5 and #6 are shown Figure 2. The different flow domains of experiments #4, #5 and #6 are clearly identified in absorption images: capillary and viscous fingering are observed for tests #4 and #6 respectively with a large unsaturated area and as expected, test #5 is a rather balanced flow with a small unsaturated zone. Moreover, inter-tow meso-voids resulting from strong capillary effects are apparent for test #4. In this case, the

  doi:10.5075/epfl-298799_978-2-9701614-0-0

flow front is almost flat due to the domination of homogeneous diffusion inside the tows whereas in test #6, it is less sharp since it is highly influenced by fabrics layup resulting in an irregular meso-porosity network. By employing a contrast agent, a high resolution and fluid/fabric contrast are obtained in absorption images whereas little information can be extracted from refraction and scattering images in which the flow front is disturbed by the fluid composition, affecting the refraction properties.

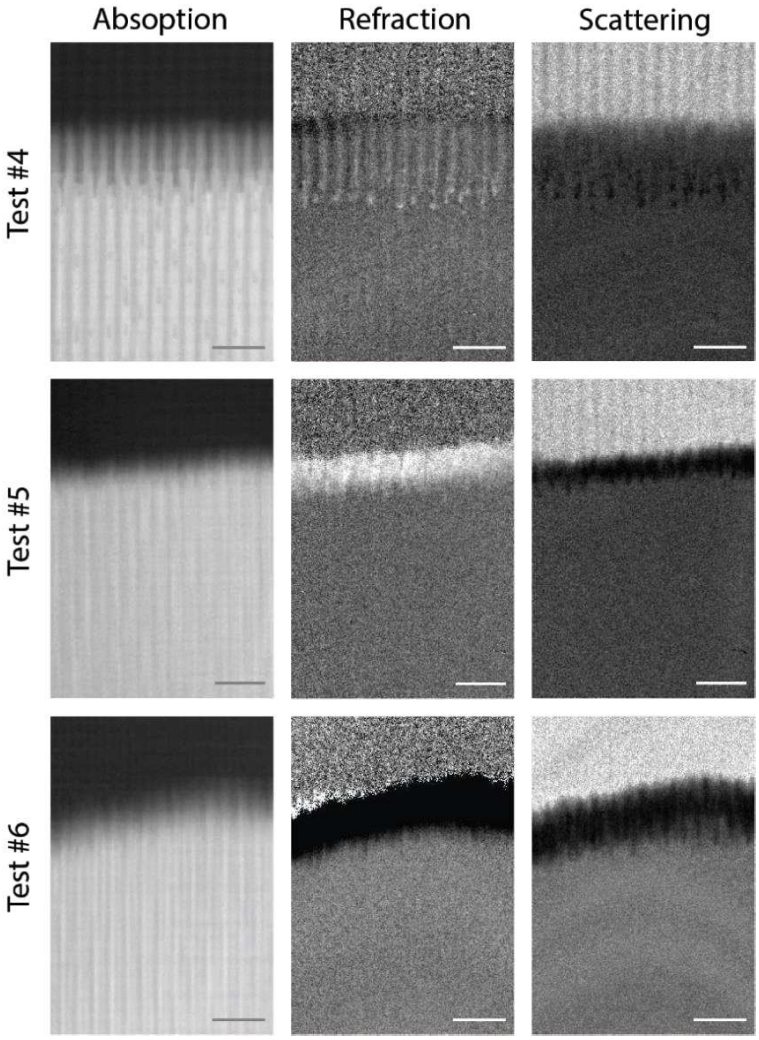

Figure 2. Absorption, refraction and scattering images obtained for tests #4, #5 and #6. The scale bar corresponds to 5 mm.

In addition, the fabric architecture and in particular the presence of horizontal glass stitches was found to significantly affect the flow pattern. In the capillary-driven case, those fiber bundles create “pools” which lead to macro-void entrapment as shown in the sequence of images in Figure 3 and explained in Figure 4. In the viscous case, they form large porosity areas within the fibrous preform leading to a stabilization of the flow as shown in Figure 4.

1017/1151 ©2022 Teixido et al. doi:10.5075/epfl-298799_978-2-9701614-0-0 published under CC BY-NC 4.0 license

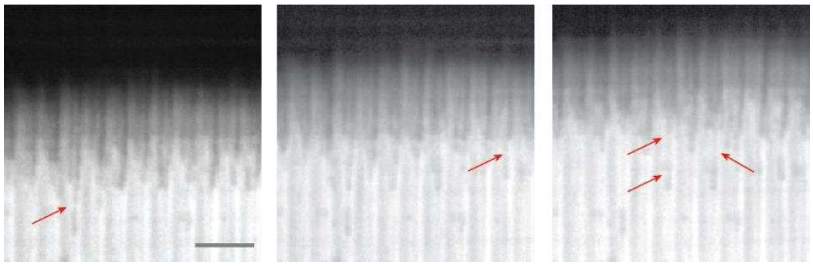

Figure 3. Macro-void formation in impregnation #4. From left to right the images correspond to the times 614.7 s, 634.7 s and 643.8 s. Red arrows show some examples of void entrapment due to the horizontal stitches. The scale bar corresponds to 4 mm.

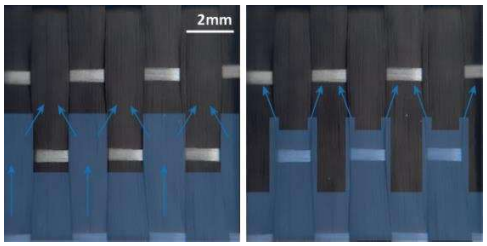

Figure 4. Influence of the fabric architecture on capillary (right) and viscous (left) flow patterns.

3.3 Visualization methods comparison

We evaluated the visualization of flow patterns by X-ray phase contrast imaging (impregnation carried out with a model fluid) and by conventional X-ray radiography (using a ZnI_2-based contrasting solution). Figure 5 shows the histograms of the different images presented in Figures 1 and 2 for tests #2 and #5. For the absorption image, peaks of dark and light grays are clearly differentiated with the use of contrasting agents. Moreover, the pixel intensity range for fluid and fabric is narrower when compared to the scattering images histogram which leads to a better differentiation between materials. This simplifies the image interpretation and analysis since the objective is to build the dynamic saturation curve for each experiment following the grayscale analysis method presented in (12) and thereupon model the progressive saturation with a two-phase flow model adapted from soil science. Finally, Table 3 presents the main advantages and disadvantages of the two approaches.

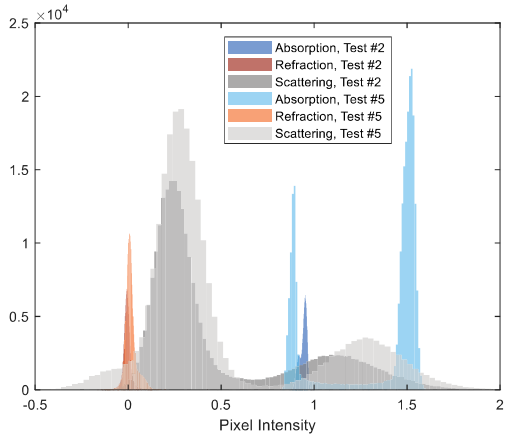

Figure 5. Histogram of absorption, refraction and scattering images of tests #2 and #5.

Table 3: Advantages and disadvantages between visualization methods.

	Advantages	Disadvantages
X-ray phase contrast	Scattering images can be used to track flow paths at a real scale even with conventional resins. Additional information of the flow type can be extracted from refraction images.	Scattering image resolution is not sufficient to extract flow patterns. For example, capillary fingering is hindered by the scattering images. Time of acquisition can be too long for fast flows observation.
X-ray transmission	Fine detail is obtained and the flow patterns can be clearly depicted. Since the grating movement specific for scattering and refraction images is not needed, the time of acquisition can be reduced.	Need of contrasting agents to visualize flow patterns, slightly modifying the fluid properties.

4. Conclusions

The present results show that conventional X-ray radiography is a suitable technique for in-situ flow analysis for Liquid Composite Molding studies and in particular for non-translucent preforms. Despite the low density of carbon fabrics, by adding contrast agent we were able to enhance the fluid/fabric contrast in absorption images and elucidate fluid paths at a real impregnation rate with a satisfactory resolution. The flow front for different impregnation conditions was successfully tracked for a unidirectional carbon preforms. Capillary to viscous fingering were clearly identified and the location and shape of meso-porosity for the capillary case was even observed. However, some hurdles need to be overcome to fully complete the flow analysis: (i) for viscous flows, the flow displacement per image acquisition can be too significant leading to a slight error when building the saturation curve, to overcome this, it is sought to reduce the time of acquisition; (ii) a complete analysis of the final saturation state (accurate measurement of the residual porosity) is needed to properly describe the flow behavior for the modeling; (iii) micro-void formation and location is hardly identified with this method.

Acknowledgements

This work was supported by the Swiss National Science Foundation (SNF n° 200021_182669).

5. References

1. Teixidó H, Staal J, Caglar B, Michaud V. Capillary Effects in Fiber Reinforced Polymer Composite Processing: A Review. Frontiers in Materials. 2022;9:1–24.

2. Michaud V. A Review of Non-saturated Resin Flow in Liquid Composite Moulding processes. Transport in Porous Media. 2016;

  doi:10.5075/epfl-298799_978-2-9701614-0-0

3. Konstantopoulos S, Fauster E, Schledjewski R. Monitoring the production of FRP composites : A review of in-line sensing methods. Express Polymer Letters. 2014;8(11):823–40.

4. Caglar B, Esposito W, Nguyen-Dang T, Laperrousaz S, Michaud V, Sorin F. Functionalized Fiber Reinforced Composites via Thermally Drawn Multifunctional Fiber Sensors. Advanced Materials Technologies. 2021;6(3):1–8.

5. Thomas S, Bongiovanni C, Nutt SR. In situ estimation of through-thickness resin flow using ultrasound. Composites Science and Technology. 2008;68(15–16):3093–8.

6. Konstantopoulos S, Grössing H, Hergan P, Weninger M, Schledjewski R. Determination of the unsaturated through-thickness permeability of fibrous preforms based on flow front detection by ultrasound. Polymer Composites. 2018;39(2):360–7.

7. Endruweit A, Glover P, Head K, Long AC. Mapping of the fluid distribution in impregnated reinforcement textiles using Magnetic Resonance Imaging : Application and discussion. Composites Part A. 2011;42(10):1369–79.

8. Bréard J, Saouab A, Bouquet G. Dependence of the reinforcement anisotropy on a three dimensional resin flow observed by X-ray radioscopy. Journal of Reinforced Plastics and Composites. 1999;18(9):814–26.

9. Vilà J, Sket F, Wilde F, Requena G, González C, Llorca J. An in situ investigation of microscopic infusion and void transport during vacuum-assisted infiltration by means of X-ray computed tomography. Composites Science and Technology. 2015;119:12–9.

10. Castro J, Sket F, González C. S-XCT experimental determination of local contact angle and meniscus shape in liquid moulding of composites. 2020;199(April).

11. Castro J, Sket F, Helfen L. In situ local imaging and analysis of impregnation during liquid moulding of composite materials using synchrotron radiation computed laminography. Composites Science and Technology. 2021;215(August).

12. Teixidó H, Caglar B, Revol V, Michaud V. In-operando dynamic visualization of flow through porous preforms based on X-ray phase contrast imaging. Composites Part A: Applied Science and Manufacturing. 2021;149.

13. Gresil M, Revol V, Kitsianos K, Kanderakis G. EVITA Project : Comparison Between Traditional Non-Destructive Techniques and Phase Contrast X-Ray Imaging Applied to Aerospace Carbon Fibre Reinforced Polymer. Appl Compos Mater. 2017;24:513–24.

14. Sket F, Enfedaque A, Alton C, González C, Molina-Aldareguia JM, Llorca J. Automatic quantification of matrix cracking and fiber rotation by X-ray computed tomography in shear-deformed carbon fiber-reinforced laminates. Composites Science and Technology. 2014;90:129–38.

